



Design and fabrication of a thermoelectric nanowire characterization platform and nanowire assembly by utilizing dielectrophoresis

Zhi Wang*, Michael Kroener¹, Peter Woias²

Laboratory for Design of Microsystems, Department of Microsystems Engineering – IMTEK, University of Freiburg, Georges-Koehler-Allee 102, D-79110 Freiburg, Germany

ARTICLE INFO

Article history:

Received 31 August 2011

Received in revised form 28 February 2012

Accepted 28 February 2012

Available online 7 March 2012

Keywords:

TNCP

Thermoelectric nanowires

Dielectrophoresis

ABSTRACT

We demonstrate the fabrication of a novel micromachined Thermoelectric Nanowire Characterization Platform (TNCP) which will be utilized to characterize the thermoelectric properties of a single thermoelectric Bi₂Te₃ nanowire. The TNCP is composed of two adjacent, symmetric and suspended Si cantilevers with a length of 1000 μm, a width of 100 μm and a thickness of 10 μm. Microheaters, temperature sensors and electrodes are fabricated on both cantilevers. Furthermore, a V-groove is integrated on the tip of each cantilever, in order to accommodate one single nanowire inside. The integration of the single nanowire onto the TNCP is conducted by means of dielectrophoresis (DEP) in combination with a controlled deposition and evaporation of a water droplet where the nanowires are dispersed. In addition to the DEP application, surface modifications are applied to form hydrophilic and hydrophobic surfaces on different parts of the cantilevers, to improve the water droplet deposition. In the end, one single nanowire is successfully integrated in the V-grooves bridging the cantilevers and ready for the further thermoelectric properties measurements. Within a series of 200 experiments, approximately 10% of them are successfully observed with one nanowire situated in the V-grooves as desired. The optimal applied voltage and frequency parameters for the DEP deposition process are in the range from 5 V to 8 V, and from 150 kHz to 8 MHz respectively.

© 2012 Elsevier B.V. All rights reserved.

1. Introduction

Quasi-one-dimensional nanostructures, such as nanowires, nanotubes, nanorods have widely drawn attentions not only in the scientific, but also in the industrial field, owing to their infinitesimally small dimensions and unique properties. Especially, nanowires are becoming more and more attractive for a variety of device applications including field-effect transistors [1,2], nanosensors [3], photodetectors [4] and so on. Within this trend, superior thermoelectric nanowires, made from Bi₂Te₃ or Sb₂Te₃, are considered to play a major role in the design of thermoelectric power generators with improved conversion efficiency [5,6].

The so-called “figure of merit” (denoted as ZT) indicates the thermoelectric efficiency of every thermoelectric material which is formularized as follows:

$$ZT = \frac{\sigma \cdot S^2}{\kappa} T \quad (1)$$

where σ is the electrical conductivity, S is the Seebeck coefficient and κ is the thermal conductivity of the thermoelectric material. Eq. (1) tells us that the ZT value can only be calculated for a nanowire, when σ , S and κ are measured on the same single specimen. However, so far the majority of previous research was made to measure merely one or two of the three parameters, with nanowires formed in bundles, mats or arrays [7,8]. Moreover, variations of the nanowire geometry, crystallographic structure or composition in nanowire arrays or bundles make the ensemble measurements unreliable for fundamental research on the underlying physical mechanism of the thermoelectric charge carrier transport. For an understanding of the thermoelectric properties, measurements on single nanowires are required to investigate the precise influence of nanowire diameter, length, crystallographic structure and chemical composition. Therefore, our research is focused on developing a platform to determine σ , S and κ concurrently on one single nanowire. For this purpose, after the fabrication of the TNCP, a technique was developed that allows: firstly, to assemble a single nanowire on a specific position of the TNCP; and secondly, to establish a well-defined thermal and electrical connection.

To date, diverse methods have been developed for nanowire assembly ranging from Langmuir–Blodgett technique [9], optical tweezers [10–13], electric field-assisted alignment (DEP) [14–19] and fluidic directed assembly [20] to the direct growth of nanowires

* Corresponding author. Tel.: +49 761 203 7475; fax: +49 761 203 7492.

E-mail addresses: zhi.wang@imtek.de (Z. Wang), michael.kroener@imtek.de (M. Kroener), woias@imtek.de (P. Woias).

¹ Tel.: +49 761 203 7584; fax: +49 761 203 7492.

² Tel.: +49 761 203 7591; fax: +49 761 203 7492.

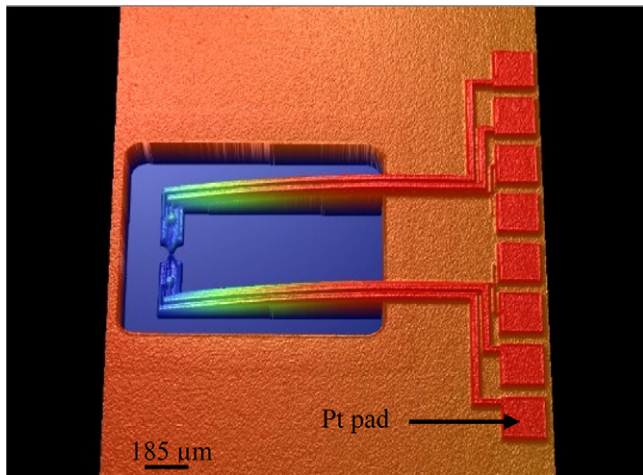


Fig. 1. TNCP profile measured by a white light interferometer.

on the pre-fabricated device [21]. Among these methods, DEP has been adopted to perform nanowire alignment in this study, because it can be used under ambient conditions without expensive equipment. Nanowires are suspended in a liquid medium, and then dielectrophoresis is used to direct and move the nanowires by means of electrical fields. The guiding field is generated by applying an AC voltage to a specific DEP electrode on the TNCP cantilevers. The applied AC voltage and frequency have a significant impact on the behavior of the nanowire inside the electric field.

2. TNCP design, modeling and fabrication

2.1. Design and modeling

The TNCP is comprised of two symmetric and facing Si cantilevers which are 1000 μm long, 100 μm wide and 10 μm thick, as shown in Fig. 1. Because the nanowires have different lengths and will be assembled on the TNCP by bridging the two cantilevers, the gap between the tips of the two cantilevers is varied from 10 to 25 μm . The cantilevers are designed as free-standing structure in order to provide a sufficient thermal insulation of the nanowire from the silicon substrate as a prerequisite for a precise measurement of the thermal conductivity κ .

Each cantilever carries a meander-shaped structure made of platinum (Pt) which has a total length of 570 μm , a width of 1.5 μm and a thickness of 200 nm. For the Seebeck coefficient measurements this Pt resistor serves not only as a microheater to establish a temperature difference between the cantilevers, hence, over the aligned nanowire, but also as a temperature sensor to detect the actual temperature on the cantilevers (Fig. 2). The Pt resistors are connected to 185 $\mu\text{m} \times 185 \mu\text{m}$ Pt bond pads on the substrates via 1400 μm long, 30 μm wide and 200 nm thick Pt leads on the long suspended cantilevers. The Pt leads are designed much wider than the Pt meander structure, and as such the resistance of Pt meander structure is a lot higher than that of the Pt leads. In this way, the majority of the voltage drop and heating effect is generated by the Pt meander structure and located at the cantilever tip, as desired. Symmetric V-grooves are designed on each cantilever tip via anisotropic etching in order to accommodate the ends of a single nanowire bridging the two cantilevers. The width and depth of the V-grooves are 2 μm and 1.41 μm , respectively. Four electrodes are deposited on the bottom of each V-groove for the latter four-point measurement of the electrical conductivity σ and a 3ω approach [22] for the κ measurement (see Fig. 2 inset). Also, two electrodes are designed symmetrically on each cantilever for DEP.

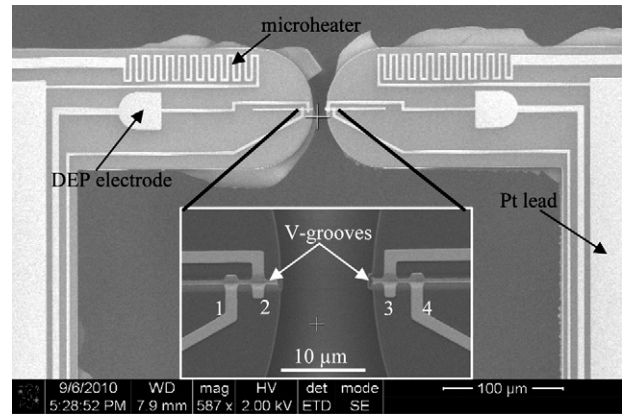


Fig. 2. SEM image of the cantilever tips. Meander shaped Pt resistor works not only as a heater but also as a temperature sensor to probe the temperature on the cantilevers. An electrical field is generated on the DEP electrodes for the nanowire assembly. Inset: Four electrodes are designed on the bottom of the V-grooves in order to measure the thermal and electrical conductivity.

Additionally, the shape of cantilever tips is designed in three different types, as shown in Fig. 3. For nanowire assembly, it is useful to investigate how the liquid droplet, which contains nanowires inside, can be guided on the cantilever tips based on different shapes.

As mentioned before, the meander-shaped Pt structure is designed as the microheater to establish the temperature gradient across the two cantilevers. Our idea is to heat up the left cantilever by applying current on the microheater, while the other cantilever remains at room temperature. Due to the temperature gradient, a voltage drop is expected to be produced on the thermoelectric nanowire. In such way, the Seebeck coefficient can be measured by using the equation $S = \Delta V / \Delta T$. Therefore, it is necessary to determine the heat distribution on the cantilever and also to confirm that the heat generation is focused on the Pt meander structure, not on the Pt leads. For this reason, a 2D model as shown in Fig. 4 is used for thermal FEM simulations with ANSYS. In this simulation, the reference temperature has been set to the room temperature (293 K). The temperature on the bottom of the TNCP chip is also fixed to room temperature. We assume the chip holder, in which the TNCP will be mounted in a final stage to be isothermal here. For the electrical boundary condition, a voltage of $U = 0.5 \text{ V}$ is applied to the microheater via the according rectangular bond pads in the model. From that, a temperature difference of 4.3 K is created between the two ends of the nanowire which is fairly sufficient for the measurement. Most of the heat is generated directly on the meander structure as intended with this design. We can see from the simulation that the left cantilever is heated up very homogeneously around the heating structure, while the right cantilever remains unaffected.

In the TNCP design, there is an insulation layer stack of $\text{SiO}_2/\text{Si}_3\text{N}_4$ between the metal layer and the Si layer in order to avoid electrical and thermal leakage currents. However, as the current is applied on the microheater, a small amount of heat will penetrate the insulation layer to the Si layer which might cause cantilever bending due to the different coefficients of thermal expansion between the $\text{SiO}_2/\text{Si}_3\text{N}_4$ layer stack and the Si layer. Thus, another FEM simulation has been conducted to determine the mechanical deflection of the long suspended cantilever beam in advance of fabrication. The issue is extraordinarily vital for the TNCP design and the nanowire assembly, because the displacement of the cantilever could damage the assembled single nanowire, and would as well make the assembly process more difficult. The simulation results show that the maximum deflection is located on the edge of the cantilever (as shown in the red area), which is approximately 38 nm (see Fig. 5). In this study, the thermoelectric nanowires have

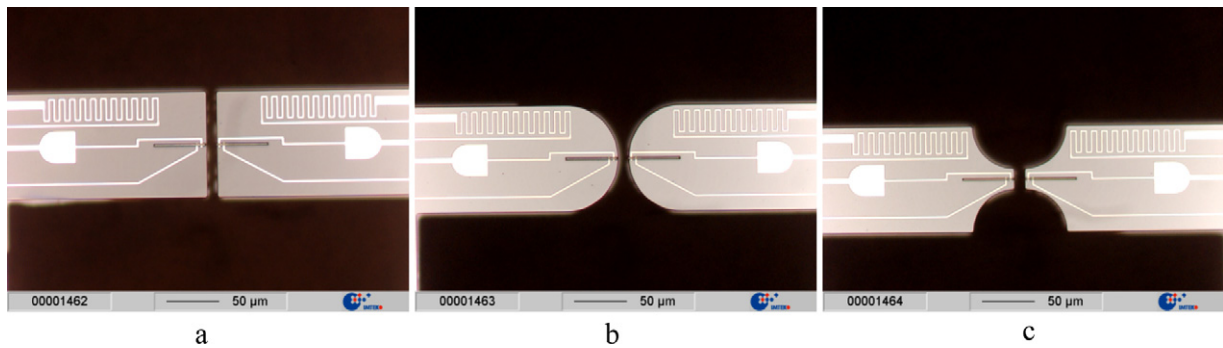


Fig. 3. Three types of cantilever tips for liquid guiding.

a diameter in the range between 200 nm and 300 nm and a length from 20 μm to 40 μm . The deflection of the cantilever beam is by far smaller than the dimensions of the nanowire, and hence can be neglected. Also, from our experiments described in Section 3.2.2, we were not experiencing any problems in NW deposition by using the microheater structures to accelerate the assembly process.

2.2. TNCP fabrication

The batch-fabrication of the TNCP is started with 100 mm diameter silicon-on-insulator (SOI) wafers with a 380 μm thick handle Si layer, a 1 μm thick buried SiO_2 layer and a 10 μm thick device Si layer on the top. First, 300 nm SiO_2 and 100 nm Si_3N_4 layers are deposited on both sides of the SOI wafer by means of wet thermal oxidation and low pressure chemical vapor deposition (LPCVD), respectively (Fig. 6a). The $\text{SiO}_2/\text{Si}_3\text{N}_4$ stack layer serves as a mask for the latter Si anisotropic wet etching. Two photolithography steps are executed on both sides and the photoresist pattern is transferred to the $\text{SiO}_2/\text{Si}_3\text{N}_4$ layer by reactive ion etching (RIE). After the RIE step, the V-grooves and cavities on the surface and the bottom side, respectively, are formed via wet chemical etching with 30% potassium hydroxide (KOH) solution at a temperature of 60 $^\circ\text{C}$. The etch rate of Si by KOH is calculated to be around 0.33 $\mu\text{m}/\text{min}$. As SiO_2 is also slightly attacked by KOH, tetramethylammonium hydroxide (TMAH), which will precisely etch-stop at the buried oxide layer, is employed to substitute KOH at the end of the bottom-cavity formation (Fig. 6b). Next, hydrofluoric acid (HF) is used to remove the $\text{SiO}_2/\text{Si}_3\text{N}_4$ layers on both sides including the buried oxide layer (Fig. 6c). Afterwards, wet thermal oxidation and LPCVD are used to grow a new $\text{SiO}_2/\text{Si}_3\text{N}_4$ layer stack on both sides of

the membrane. Due to the uniform $\text{SiO}_2/\text{Si}_3\text{N}_4$ layers on both sides of the membrane, the internal layer stress is compensated. This prevents an unwanted stress-induced bending of the released cantilever. Besides, as mentioned before, the $\text{SiO}_2/\text{Si}_3\text{N}_4$ stack layer also effectively prevents the current leakage while the current is flowing in the Pt resistor. After the deposition of a 10 nm titanium (Ti) adhesion layer and a 200 nm Pt layer on the top by means of radio-frequency (RF) sputtering, the third photolithography step is applied to pattern this metal layer via ion beam etching (IBE), as shown in Fig. 6d. Another photolithography step is utilized to pattern the wafer surface for the deep reactive ion etching (DRIE) process that shapes the cantilevers (Fig. 6e). By using spray-coating of a photoresist, the backside $\text{SiO}_2/\text{Si}_3\text{N}_4$ stack layer of the cantilever is protected from the next RIE step (Fig. 6f). Without this protection layer, it is found that the RIE etching gas passes through the already etched region to the backside of the cantilevers and removes the $\text{SiO}_2/\text{Si}_3\text{N}_4$ stack layer on the backside which is detrimental for the stress compensation purpose and causes a bending problem of the cantilever after its release. Using RIE on the top side, the cantilevers are finally released from the remaining $\text{SiO}_2/\text{Si}_3\text{N}_4$ stack layer and the photoresist is stripped by Diener Tetra oxygen plasma (Fig. 6g).

After the SOI wafer dicing, approximately 600 TNCP chips with dimensions of 2 mm \times 3 mm (Fig. 6, inset) are produced on one SOI wafer. However, a large amount of Si particles are observed sticking firmly to the surface of the TNCP after the wafer dicing, as shown in Fig. 7a. These Si particles are presumably generated during the wafer dicing and might cause short-circuit when current is applied to the metal layers. Therefore, a short time (≈ 90 s) dipping of the chips into a 30% KOH solution is applied to remove the Si particles, as shown in Fig. 7b.

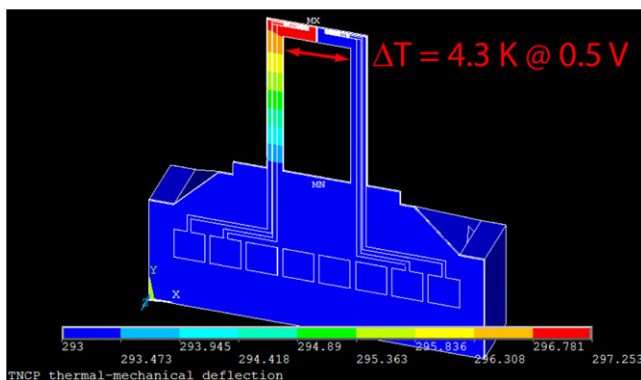


Fig. 4. FEM simulation of heat distribution on the left arm of the TNCP. The electrical voltage of 0.5 V is applied to the micro heater structure of the left cantilever ($P = 0.75$ mW). The reference temperature is 293 K. A temperature difference of 4.3 K is generated between the left and right cantilever arms, which is sufficient to measure the properties of a single NW in between.

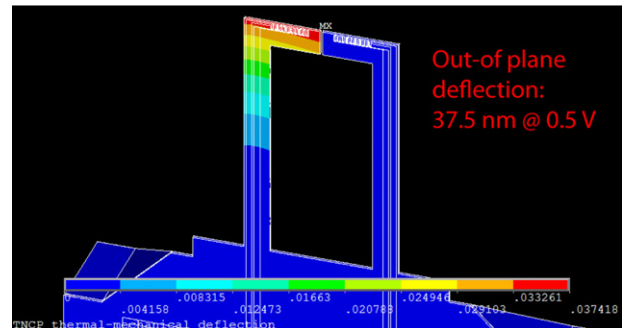


Fig. 5. FEM simulation of the thermal-mechanical deflection of the cantilever. The applied electrical power is 0.75 mW, the reference temperature 293 K. The maximum deflection at the cantilever tip (out-of-plane bending) is approximately 38 nm, which is negligible.

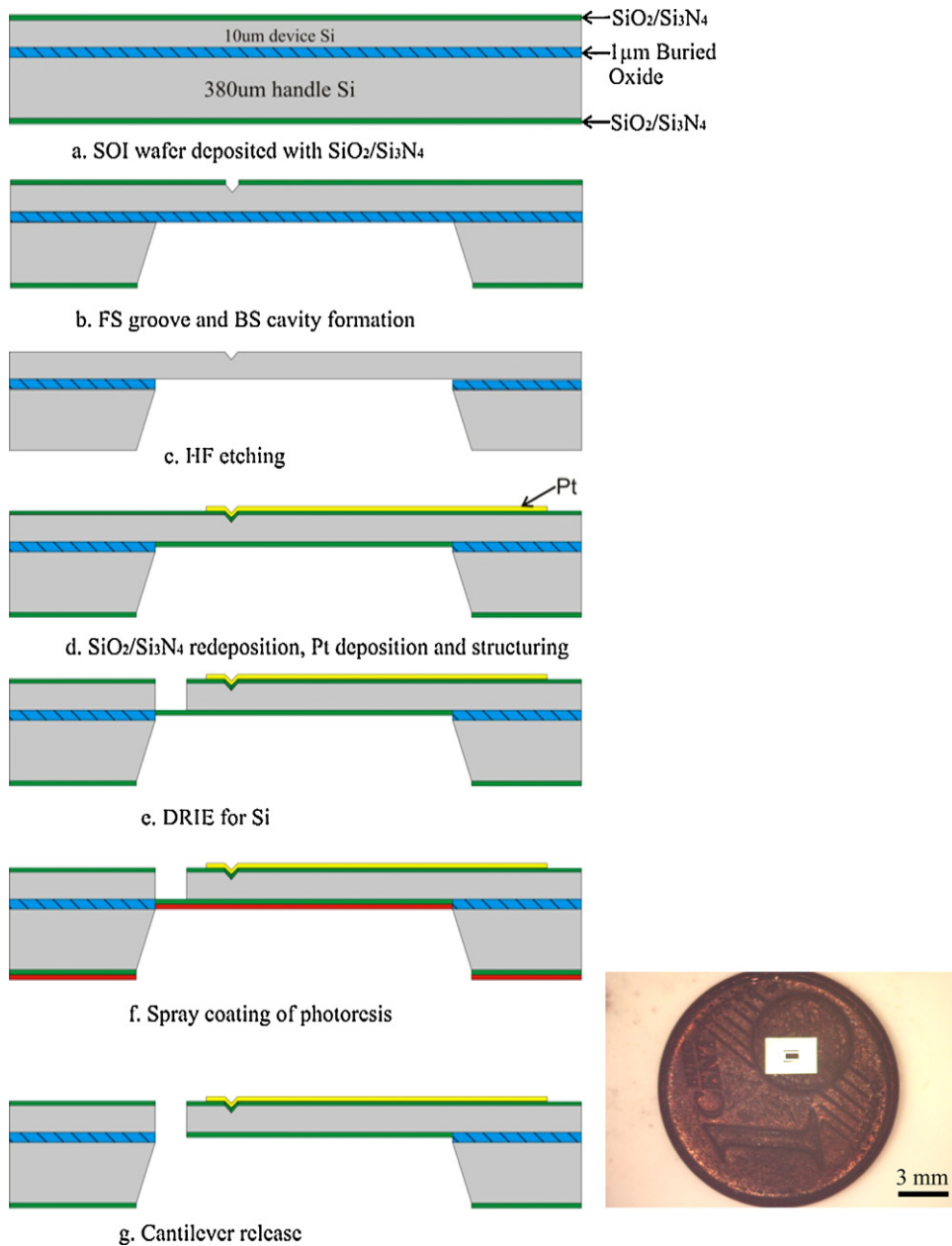


Fig. 6. Fabrication process of the TNCP. Inset: one 2 mm × 3 mm TNCP comparing to one Euro cent coin.

3. Nanowire assembly

3.1. Dielectrophoresis

Dielectrophoresis is becoming increasingly popular because it can be used to manipulate micro- or nanoparticles, such as nanowires, nanotubes and nanorods which are dispersed in a liquid medium [16–18]. Dielectrophoresis is a contact-free and non-destructive technology for particle manipulation. The definition of the dielectrophoretic force was first put forward by Pohl in 1951. An uncharged object will experience a translational force, \vec{F} , when it is brought into an inhomogeneous electric field, \vec{E} . The force is proportional to the square value of the electric field [23,24]. In more detail, if a neutral particle experiences an external electric field, this will develop an induced dipole moment within the particle which is expressed as follows:

$$\vec{p} = q \cdot \vec{d} \quad (2)$$

where d is the displacement vector and q is the charge of the dipole. The induced dipole moment \vec{p} is highly dependent on the electric field strength and the polarizability of the material.

Due to the external nonuniform electrical field, there exists a net force on the induced dipole, as shown in Eq. (3). This force is proportional to its dipole moment and the gradient of the electric field.

$$\vec{F} = \vec{p} \cdot \nabla \vec{E} \quad (3)$$

By adding up the force exerted on all the induced dipoles within the particle, the dielectrophoretic force on the particle can be extrapolated. Here, the electric field can either be generated by a DC voltage or an AC voltage that both can produce nonuniform electric fields. In addition to the DEP force, the induced dipoles also result in a torque which aligns the particles to the direction of the external electric field [25,26]. Indeed, the polarizability of the particle and the medium are playing a major role for the application of dielectrophoretic forces. Generally, if the polarizability of the particle α_p

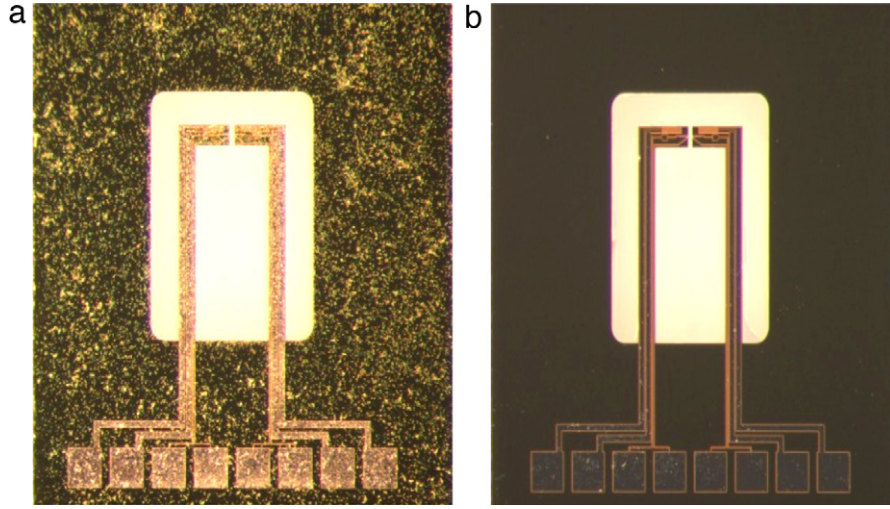


Fig. 7. TNCP cleaning by KOH dip. (a) Before KOH dip and (b) after KOH dip.

is greater than the polarizability of the medium α_m , the particle will be attracted toward the region with the higher electric field gradient. This is named as positive dielectrophoresis. In contrary, when α_m is higher than α_p , the particle will be repelled from the region of higher electric field gradient to the region of lower electric field gradient, which is called negative dielectrophoresis. Therefore, it is necessary to note that the movement of particles by DEP force is not dependent on the direction of the external electric field, but only on the electric field gradient.

In this work, the assembly of a single nanowire has been studied by using the DEP effect with different applied voltages and frequencies. For cylindrical particles, as assumed for thin, long nanowires, which are suspended in a fluid medium, the dielectrophoretic force can be written as [27]:

$$F_{\text{DEP}} = \frac{2L\pi r^2}{3} \varepsilon_m \text{Re}[K(\omega)] \cdot (\nabla |E|^2) \quad (4)$$

where r and L are the radius and length of the nanowire, respectively. ε_m is the permittivity of the medium, E is the time-varying applied electric field, and $K(\omega)$ is the Clausius Mossotti factor for cylindrically shaped particles as a complex number. The real part of $K(\omega)$ can be expressed as follows [27]:

$$\text{Re}[K(\omega)] = \text{Re} \left[\frac{\varepsilon_p^*(\omega)}{\varepsilon_m^*(\omega)} - 1 \right] = \frac{\omega^2 \varepsilon_p \varepsilon_m + \sigma_p \sigma_m}{\omega^2 \varepsilon_m^2 + \sigma_m^2} - 1 \quad (5)$$

where ε_p is the permittivity of the particle, ω is the angular frequency of the applied AC voltage, σ_p and σ_m are the electrical conductivity of the particle and of the fluid medium, respectively. The ratio $[\varepsilon_p^*(\omega)/\varepsilon_m^*(\omega) - 1]$ can be changed by varying the frequency ω of the applied alternating voltage. When the ratio exceeds zero, which makes the real part of the Clausius Mossotti factor $\text{Re}[K(\omega)] > 0$, positive DEP force is exerted on the nanowires. In contrast, when the ratio becomes smaller than zero, i.e. $\text{Re}[K(\omega)] < 0$, the negative DEP force arises and moves the nanowire toward the region with minimum electric field (Fig. 8). Clearly, the angular frequency ω of the applied AC voltage has a great effect on the DEP force according to Eq. (5). Eqs. (6) and (7) depict how the frequency affects the DEP force [28].

$$\lim_{\omega \rightarrow \infty} \text{Re}[K(\omega)] = \frac{\varepsilon_p - \varepsilon_m}{\varepsilon_m} \quad (6)$$

$$\lim_{\omega \rightarrow 0} \text{Re}[K(\omega)] = \frac{\sigma_p - \sigma_m}{\sigma_m} \quad (7)$$

Obviously, when the angular frequency ω tends to infinity, DEP force is dominated by the nanowire permittivity ε_p and the solution

permittivity ε_m . On the other hand, when the angular frequency ω tends to zero, the electrical conductivities of the nanowire and solution, σ_p and σ_m , become dominant and thereby determine the DEP force.

3.2. Experimental details

3.2.1. Liquid medium selection

In the beginning, isopropanol alcohol (IPA) solution is used to suspend the Bi_2Te_3 nanowires. However, it turns out that IPA cannot form spherical droplets on the tips of the cantilevers and distributes rapidly along the cantilevers due to the surface tension. The other drawback of IPA is that it evaporates too fast to benefit from the DEP force. Consequently, DI water is adopted to substitute IPA solution. By using an aqueous water solution, spherical droplets with nanowires inside can be readily generated on the tips of the cantilevers.

3.2.2. Nanowire assembly process

In our work, a single thermoelectric Bi_2Te_3 nanowire (Fig. 9) has been accurately integrated into the $2\text{ }\mu\text{m}$ wide V-grooves at the tips of the cantilevers. The nanowires have a diameter ranging from 200 nm to 300 nm and a length between $20\text{ }\mu\text{m}$ and $40\text{ }\mu\text{m}$. By using Eqs. (5) and (6), and with the relative permittivity of a Bi_2Te_3 nanowire ($\varepsilon_p = 58$ [29]) and of water ($\varepsilon_m = 80$), respectively, $\text{Re}[K(\omega)] = -0.275$ at a frequency of 6 MHz . This implies that the Bi_2Te_3 nanowires will be dragged to regions with lower electric field strength. According to Eq. (4), the maximum DEP force

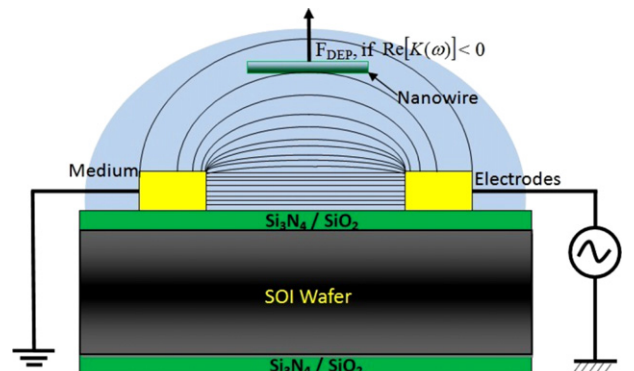


Fig. 8. DEP force on a nanowire in a liquid for $\text{Re}[K(\omega)] < 0$.

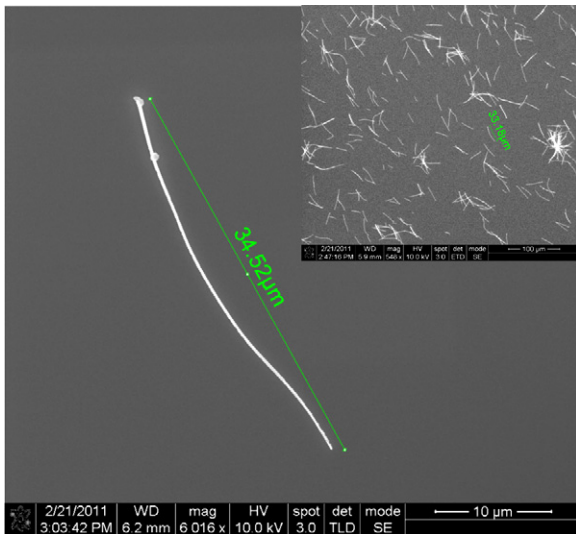


Fig. 9. SEM image of a single Bi_2Te_3 nanowire which presumably possesses superior thermoelectric properties. Inset: a large number of nanowires dispersed on one Si wafer.

exerted on a nanowire is approximately $-44 \mu\text{N}$ which pushes the nanowire up to the dome of the droplet with an oriented direction parallel to the surface of the cantilevers and the V-grooves (Fig. 10a).

For nanowire assembly, the nanowires are suspended in DI water solution at first. The water sample is diluted so that nanowires can be separated into smaller fractions. A small droplet (50–100 nl) is dispensed on the cantilever by using a micro-scale pipette with a $200 \mu\text{m}$ diameter tip which is coated with Teflon. As time elapses, the droplet shrinks due to the evaporation. Meanwhile, the nanowires remain within the confinement given by the droplet and hover above the TNCP cantilever tips. An AC voltage is applied to generate a negative DEP force and to orient and polarize

the nanowires. The negative DEP force turns out to be advantageous for nanowire assembly. If the DEP force was positive, nanowires would be attracted randomly to the entire cantilever surface very fast, and become immobilized before they are precisely aligned. With a negative DEP force, the nanowires are forced toward the dome of the droplet, in a perfect alignment to the cantilever's V-grooves. By evaporation of the droplet, the nanowire is pulled close and close to its intended landing site. After the droplet is fully evaporated, at least one nanowire is bridging the cantilever tips, this process is demonstrated in Fig. 10a–d. The frequency of the applied AC voltage should be greater than at least 150 kHz. It is found that for frequencies below 150 kHz, a large amount of bubbles occur, which severely corrode the electrodes. This corrosion effect is related to the electrolysis of water on the DEP electrodes, which also appears for large enough DC voltages.

3.2.3. Surface modification

While performing the water droplet deposition, it is found that the water droplet easily sticks to other parts of the TNCP, not exclusively to the cantilever tips. This is because the whole TNCP surface has hydrophilic property. Therefore, the surface properties of the TNCP are selectively modified for an improved nanowire assembly. The tips of the cantilevers are at first manually coated with photoresist, as illustrated in Fig. 11. Afterwards, a 100 nm thick Teflon-like polymer layer is coated on the whole TNCP chip by means of Octafluorocyclobutane (C_4F_8) plasma. After removal of the photoresist using acetone, the cantilever tips remain hydrophilic, while all the other parts of the TNCP surface exhibit a hydrophobic behavior. This treatment considerably facilitates the deposition of water droplets onto the tips of the cantilevers.

3.2.4. Acceleration of water droplet evaporation

After the successful deposition of one water droplet on the cantilever tips, it is found that the water droplet takes a long time (4 min) to evaporate completely. This is undesired for a controlled nanowire assembly, as it allows the nanowires to move inside the

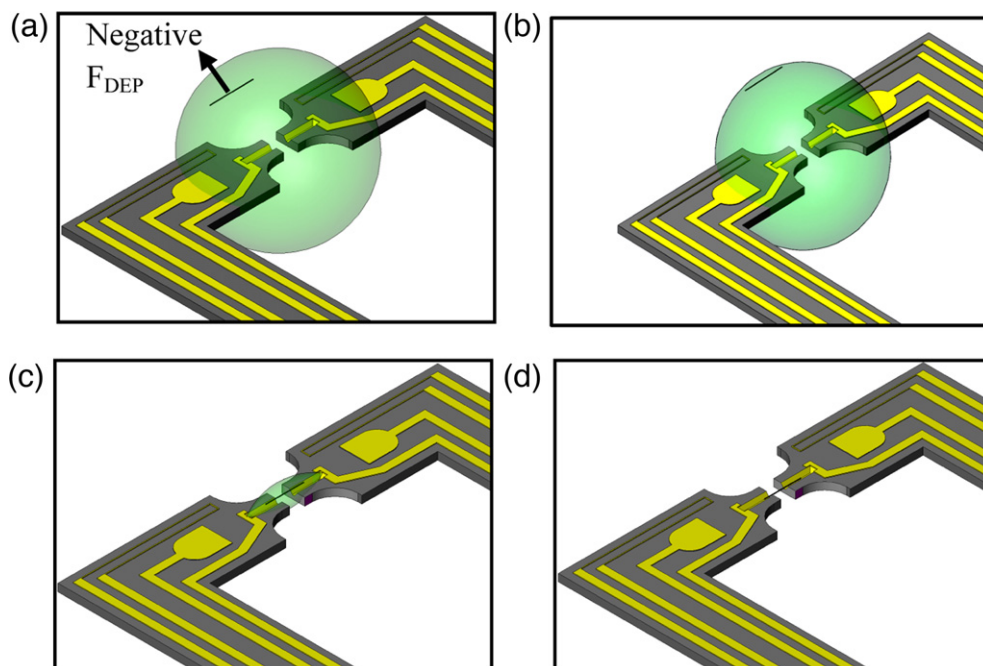


Fig. 10. Evaporation-assisted nanowire assembly. (a) A water droplet is dispensed on the tips of cantilevers; an AC voltage is applied to produce a negative DEP force in the meantime. (b) Due to the negative DEP force, the nanowire is repelled from the cantilever tips to the dome of the water droplet, and it is directed parallel to the electric field direction because of torque generated by the induced dipoles. (c) As the water droplet evaporates, the confined nanowire has less space to move. (d) Finally, the nanowire is positioned in the V-grooves after the water droplet is entirely evaporated.

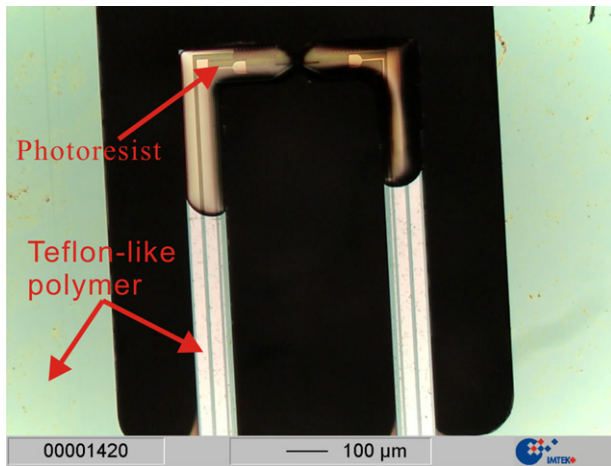


Fig. 11. Hydrophilic and hydrophobic surfaces generation by Teflon-like polymer deposition. After resist stripping, the tips of the cantilevers possess hydrophilic surface while the other parts of TNCP exhibit hydrophobic property.

droplet in an uncontrolled way, with all negative side effects, for instance, agglomeration or unwanted surface adhesion. Hence, the microheaters on the cantilever tips are used to heat up the water droplet with a total applied electrical power of 5.2 mW to reduce the dry-out time to 30 s (Fig. 12). Shortly before the complete evaporation of the droplet (after approximately 25 s), the electrical power is turned off, in order that the nanowire can be positioned into the V-grooves without any other electrical or thermal disturbances. During the heating, some bubbles are observed in the vicinity of the cantilevers, as seen in Fig. 12b and c. Proper explanation to this phenomena is that the heated water droplet is evaporating fast at a high temperature in the region of the cantilever tips, and then the evaporated water condenses again at the side walls, which are still at room temperature. As seen in Fig. 12d, the final confinement of the nanowires is taking place as expected. The remaining droplet volume after a time of 25 s is approximately 10 nl.

3.2.5. Determination of one assembled nanowire

The in situ assembly process of one nanowire cannot be readily observed under an optical microscope which is a big obstacle for the study of the assembly mechanism. Therefore, a novel method has been developed to determine the assembly success in this work. The evaporation behavior of the droplet gives an indication for the success. With nanowires inside the V-grooves the water droplet is trapped and evaporates along the nanowires due to the adhesive forces. As a consequence, the water droplet vanishes in the same horizontal line as the V-grooves (Fig. 13a). If the nanowire is not situated in the V-grooves, it can be observed in the microscope that the water droplet evaporates in another spot where the nanowire is located, but not in the horizontal line of the V-grooves. On some occasions, there is even no nanowire in the water droplet if it is many times diluted. In this case, the water droplet will coalesce at one of the cantilever tips (Fig. 13b). Therefore, the evaporation pattern of the water droplet, which is easily observed under an optical microscope gives a detailed insight into the deposition of the optically invisible nanowire. This helps to avoid time-intensive SEM inspection.

4. Results and discussion

The dielectrophoretic force used for nanowire deposition is strongly dependent on the applied AC voltage and the frequency, as seen in Eqs. (4) and (5). From the experimental results, the frequency of the applied sinusoidal signal has to be larger than 150 kHz. Otherwise, electrolysis takes place on the DEP electrodes which inhibits the nanowire deposition. When the frequency is increased from 150 kHz to 10 MHz, no significant difference has been observed for the DEP force. On the other hand, the applied peak-to-peak AC voltage plays an important role. By varying the voltage from 1 V_{pp} to 10 V_{pp}, while the frequency is fixed at 1 MHz, which is high enough to avoid electrolysis, nanowires deposition varies considerably, as depicted in Fig. 14. The results are selected from a set of twenty nanowire assembly experiments. In these experiments, the DI water solution with nanowires inside is not diluted, leading to a relatively large number of nanowires in the extracted 80 nl droplet. We assume that the extracted water droplet

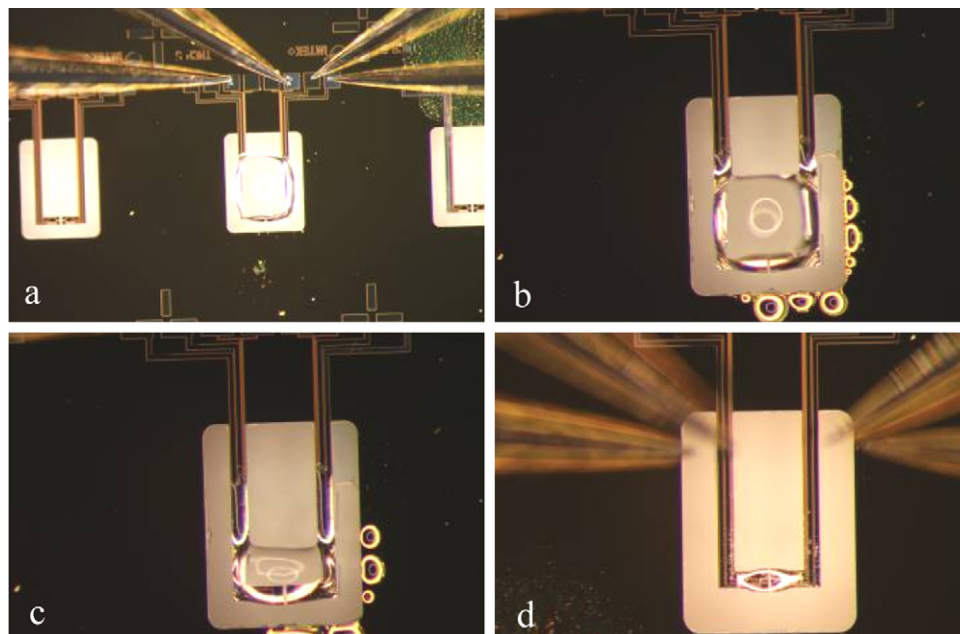


Fig. 12. Dry-out process of an 80 nl water droplet. The evaporation of water droplet is accelerated by applying an electrical power of 5.2 mW to the microheaters. The evaporation time is thereby reduced from 4 min to 30 s. Water droplet evaporation process in respect to the time, (a) 0 s, (b) 5 s, (c) 15 s and (d) 25 s.

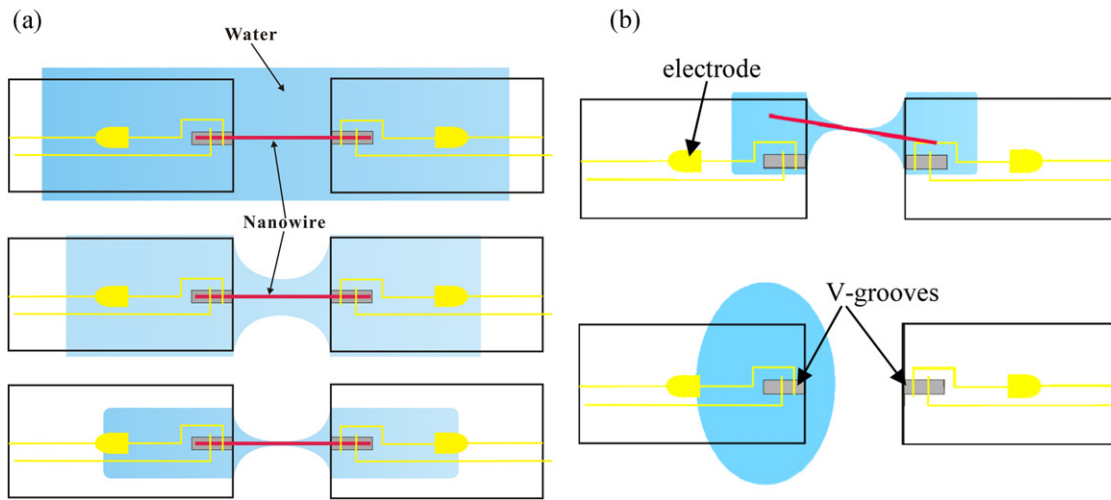


Fig. 13. Determination of the success of nanowire assembly.

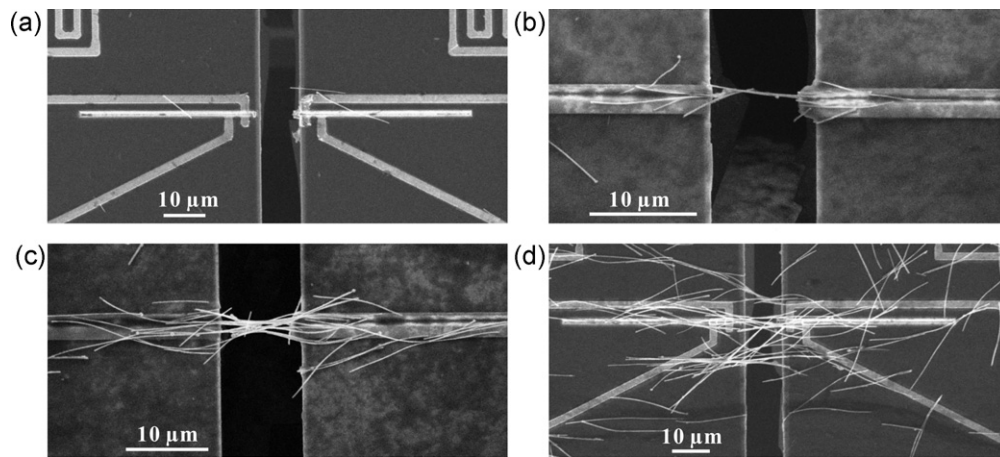


Fig. 14. SEM images showing nanowire assembly between the two cantilevers at different applied AC voltages, the applied frequency is fixed at 1 MHz (a) 1 V_{pp}, (b) 3 V_{pp}, (c) 6 V_{pp} and (d) 10 V_{pp}.

contains nearly the same amount of nanowires each time. Fig. 14a demonstrates that due to the very small applied voltage (1 V_{pp}), only few nanowires are aligned in the vicinity of the V-grooves and no bridged nanowires are observed. For a voltage of 3 V_{pp} and higher, the tips of the cantilevers where the V-grooves are located are bridged by multiple nanowires. The relation between the applied voltage and the DEP force is shown in Fig. 15. With increased voltage, the DEP force raises almost quadratically which leads to more nanowires aligned and directed above the electrodes. After the water droplet is evaporated, they are situated inside and outside the V-grooves (Fig. 14d). It is necessary to note that assembly of the nanowires could be interfered by hydrodynamic forces or Van der Waals forces. Therefore, some nanowires in Fig. 14d are not aligned in the direction of the V-grooves.

The TNCP chips with the rectangular shaped cantilever tips (Fig. 3a) have been used to perform nanowire assembly experiments with preference over the other two types. Because the rectangular cantilever tips have more surface area which can effectively hold the water droplet above (Fig. 12d). However, the water droplet has been frequently observed falling down on the other two types of cantilever tips. The deposition of a nanowire was not successful in all experiments, as the number of nanowires per

droplet, their aggregation state or deposition at unwanted positions cannot be completely excluded. However, within a series of 200 nanowire assembly experiments, about 10% were successful with one nanowire situated in the V-grooves as requested (Fig. 16). This justifies the efficiency of the combined evaporation-DEP process.

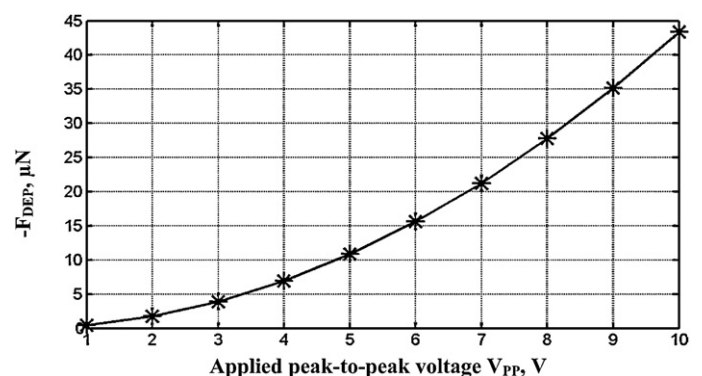


Fig. 15. DEP force with respect to the applied peak-to-peak voltage.

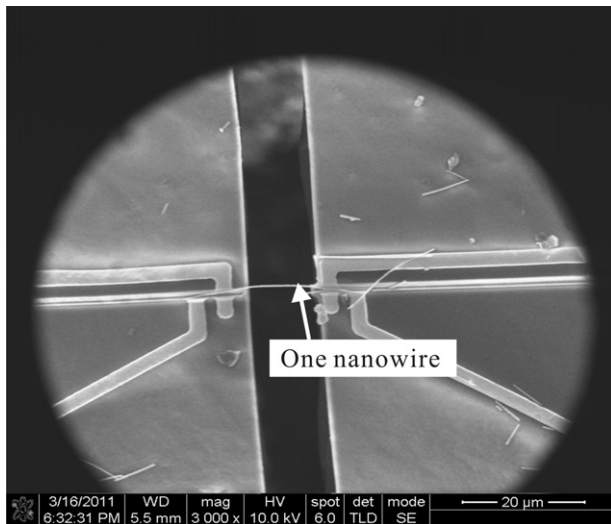


Fig. 16. Result of a successful experiment, with a single nanowire bridging the two cantilever tips. (DEP voltage: 6 V_{pp}, frequency: 8 MHz.)

After the nanowire is successfully assembled into the V-grooves, the nanowire only physically contacts the electrodes. Therefore, an electrical contact has to be generated between the nanowire and the electrodes for further measurements. As such, a small amount of Pt is deposited on top of each contact between the nanowire and electrodes by means of Scanning Electron Microscope (SEM) Focused Ion Beam (FIB) deposition. However, it is found that due to the 1.41 μm deep, 2 μm wide V-grooves, the FIB deposition takes a long time to fill out the V-grooves with Pt at each contact point, and too much Pt is wasted. Thus, a new generation of TNCP without V-grooves has been fabricated recently, while all the other parameters of the new TNCP are kept the same as in the former version. With the FIB deposited Pt on top (Fig. 17), electrical contact between the nanowire and the electrodes has been generated. Fig. 18 shows the *I*–*V* curves for a Bi₂Te₃ nanowire assembled by DEP.

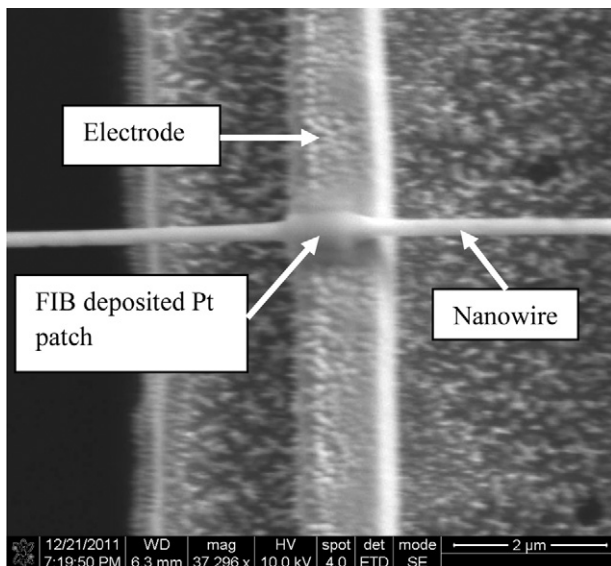


Fig. 17. FIB deposition of a small Pt patch on the top of the nanowire and electrode contact to generate electrical contact and to firmly fix the nanowire as well.

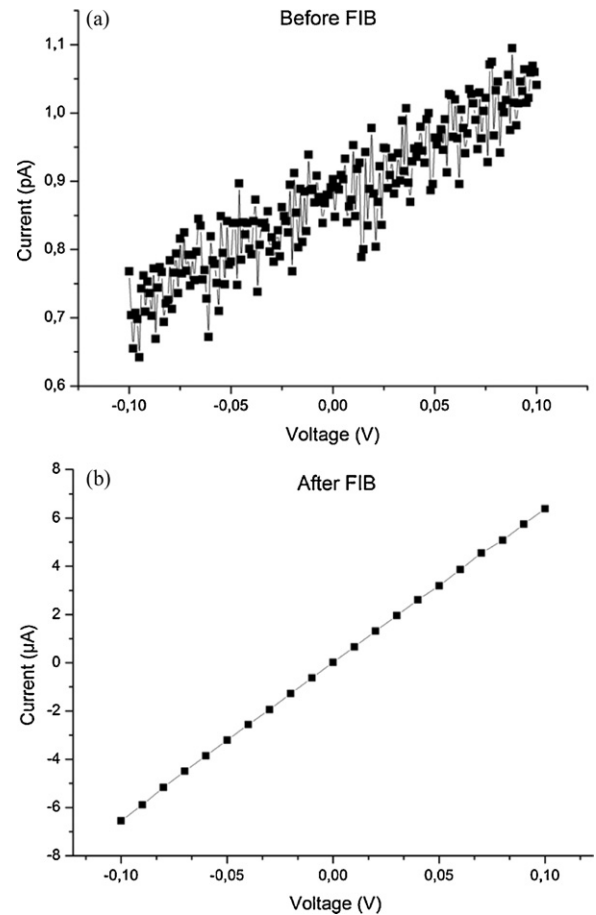


Fig. 18. (a) *I*–*V* curve before Pt-FIB deposition caused by noise and leakage currents. (b) *I*–*V* curve after Pt-FIB deposition, the applied voltage is between –100 mV and 100 mV, and the current is measured between –6.56 μA and 6.39 μA.

5. Conclusion

A novel Thermoelectric Nanowire Characterization Platform (TNCP) has been designed, modeled and fabricated. All relevant functional structures, such as microheaters, V-grooves and DEP electrodes, have been integrated on the TNCP. The microheaters can be used not only to establish the temperature difference over the aligned nanowire but also to detect the actual temperature on the cantilevers. Later it is found that the microheaters can further be used to accelerate the evaporation of the water droplet during the nanowire deposition process. The influence of the applied AC voltage and frequency on the dielectrophoretic force has been investigated. Only frequencies above 150 kHz can be utilized to perform the dielectrophoresis in order to avoid electrolysis. Referring to the voltage, it is observed that higher voltages ($>3 V_{pp}$) result in higher dielectrophoretic force which can effectively align and direct the nanowires. The best nanowire assembly results are situated in the applied DEP voltage range between 5 V and 8 V and frequency from 150 kHz to 8 MHz. The geometry, permittivity and polarizability of the nanowires have also a strong effect on the dielectrophoretic force. Especially, the polarizability determines whether the nanowires experience a positive or negative DEP force. In our work, the negative DEP force has been implemented to align a single thermoelectric Bi₂Te₃ nanowire which dragged the nanowire away from the cantilevers tips but still the nanowire was confined in the water droplet. Through the combination with droplet shrinkage during evaporation, the single nanowire has been assembled into the V-grooves bridging the two cantilevers. During

the experiments, surface modifications have been employed to facilitate the water droplet deposition and a new measure has been developed to determine the success of the nanowire assembly via the observation of the droplet evaporation scheme. Finally, electrical contact has been successfully generated between the assembled nanowire and electrodes via Pt-FIB deposition and the I – V curve of Bi_2Te_3 nanowires has been presented.

References

- [1] X. Duan, C. Niu, V. Sahi, J. Chen, J. Parce, S. Empedocles, J.L. Goldman, High-performance thin-film transistors using semiconductor nanowires and nanoribbons, *Nature* 425 (2003) 274–278.
- [2] K. Xiao, R. Li, J. Tao, E.A. Payzant, L.N. Ivanov, A.A. Puzosky, W. Hu, D.B. Geohrgan, Metastable copper-phthalocyanine single-crystal nanowires and their use in fabricating high-performance field-effect transistors, *Adv. Funct. Mater.* 19 (2009) 3776–3780.
- [3] W.U. Wang, C. Chen, K. Lin, Y. Fang, C.M. Lieber, Label-free detection of small-molecule-protein interaction by using nanowire nanosensors, *Proc. Natl. Acad. Sci. U.S.A.* 102 (2005) 3208–3212.
- [4] C.J. Novotny, E.T. Yu, P.K.L. Yu, InP nanowire/polymer hybrid photodiode, *Nano Lett.* 8 (3) (2008) 775–779.
- [5] W. Wang, F. Jia, Q. Huang, J. Zhang, A new type of low power thermoelectric micro-generator fabricated by nanowire array thermoelectric material, *Microelectron. Eng.* 77 (2005) 223–229.
- [6] H. Linke, T.E. Humphrey, M. O'Dwyer, Energy-specific equilibrium in nanowires for efficient thermoelectric power generation, in: Conference of Symposium on Materials and Technologies for Direct Thermal-to-Electric Energy Conversion, Boston, 2005.
- [7] D.S. Choi, A.A. Balandin, M.S. Leung, S.W. Chung, A. Khitun, K.L. Wang, Transport study of a single bismuth nanowire fabricated by the silver and silicon nanowire shadow masks, *Appl. Phys. Lett.* 89 (2006) 141503.
- [8] L. Shi, D. Li, C. Yu, W. Jang, D. Kim, Z. Yao, P. Kim, A. Majumdar, Measuring thermal and thermoelectric properties of one-dimensional nanostructures using a microfabricated device, *J. Heat Transfer* 125 (2003) 881–888.
- [9] D. Whang, S. Jin, Y. Wu, C.M. Lieber, Large-scale hierarchical organization of nanowire arrays for integrated nanosystems, *Nano Lett.* 3 (9) (2003) 1255–1259.
- [10] P.J. Pauzauskie, A. Radenovic, E. Trepagnier, H. Shroff, P. Yang, J. Liphardt, Optical trapping and integration of semiconductor nanowire assemblies in water, *Nat. Mater.* 5 (2006) 97–101.
- [11] S. Lee, G. Jo, T. Lee, Y. Lee, Controlled assembly of In_2O_3 nanowires on electronic circuits using scanning optical tweezers, *Opt. Exp.* 17 (20) (2009) 17491–17501.
- [12] C.H. Nam, D. Lee, D. Hong, J. Chung, Manipulation of nano devices with optical tweezers, *IJPEM* 10 (5) (2009) 45–51.
- [13] T. Yu, F. Cheong, C. Sow, The manipulation and assembly of CuO nanorods with line optical tweezers, *Nanotechnology* 15 (2004) 1732–1736.
- [14] E.M. Freer, O. Grachev, X. Duan, S. Martin, D.P. Stumbo, High-yield self-limiting single-nanowire assembly with dielectrophoresis, *Nat. Nanotechnol.* 5 (2010) 525–530.
- [15] D. Wang, R. Zhu, Z. Zhou, X. Ye, Controlled assembly of zinc oxide nanowires using dielectrophoresis, *Appl. Phys. Lett.* 90 (2007) 103110.
- [16] P.A. Smith, C.D. Nordquist, T.N. Jackson, T.S. Mayer, Electric-field assisted assembly and alignment of metallic nanowires, *Appl. Phys. Lett.* 77 (9) (2000) 1399–1401.
- [17] S. Raychaudhuri, S. Dayeh, D. Wang, E.T. Yu, Precise semiconductor nanowire placement through dielectrophoresis, *Nano Lett.* 9 (6) (2009) 2260–2266.
- [18] H.W. Seo, C. Han, S.O. Hwang, J. Park, Dielectrophoretic assembly and characterization of individually suspended Ag, GaN, SnO_2 , and Ga_2O_3 nanowires, *Nanotechnology* 17 (2006) 3388–3393.
- [19] A. Motayed, M. He, A.V. Davydov, J. Melngailis, S.N. Mohammad, Realization of reliable GaN nanowire transistors utilizing dielectrophoresis alignment technique, *J. Appl. Phys.* 100 (2006) 114310.
- [20] Y. Huang, X. Duan, Q. Wei, C.M. Lieber, Directed assembly of one-dimensional nanostructures into functional networks, *Science* 291 (2001) 630–633.
- [21] L. Shi, Mesoscopic thermophysical measurements of microstructures and carbon nanotubes, Doctoral Dissertation, 2001.
- [22] L. Lu, W. Yi, D.L. Zhang, A 3ω method for specific heat and thermal conductivity measurements, *Rev. Sci. Instrum.* 72 (7) (2001) 2996–3003.
- [23] H.A. Pohl, Dielectrophoresis, Cambridge University Press, 1978.
- [24] H.A. Pohl, K. Pollock, J.S. Crane, Dielectrophoretic force: a comparison of theory and experiment, *J. Biol. Phys.* 6 (1978) 133–160.
- [25] Y. Liu, J. Chung, W.K. Liu, R.S. Ruoff, Dielectrophoretic assembly of nanowires, *J. Phys. Chem. B* 110 (2006) 14098–14106.
- [26] S. Blatt, Dielectrophoresis of single-walled carbon nanotubes, Doctoral Dissertation, 2008.
- [27] N. Ranjan, Dielectrophoretic formation of nanowires and devices, Doctoral Dissertation, 2009.
- [28] M. Dimaki, P. Boggild, Dielectrophoresis of carbon nanotubes using microelectrodes: a numerical study, *Nanotechnology* 15 (2004) 1095–1102.
- [29] A.Y. Morsy, S.S. Fouad, E. Haschem, Optical properties of thermally deposited bismuth telluride in wavelength range of 2.5–10 μm , *Acta Phys. Pol. A* 80 (6) (1991) 819–825.

Biographies

Zhi Wang has studied electronic and information engineering at the Nanjing University of Posts and Telecommunications from 2002 to 2006 and received his bachelor's degree in Nanjing, China. From 2007 to 2009, he studied microsystems engineering at the Furtwangen University of Applied Science and received his master's degree in Furtwangen, Germany. Since 2009, he is a PhD student at the Laboratory for Design of Microsystems, Department of Microsystems Engineering – IMTEK, University of Freiburg, Germany. He is currently working for a DFG project with a focus on the “Structural and thermoelectric characterization of individual single crystalline nanowires”.

Michael Kroener is a scientific assistant at the Laboratory for Design of Microsystems, Department of Microsystems Engineering – IMTEK, University of Freiburg, Germany. From 2000 to 2004, he studied Engineering Physics at Muenster University of Applied Sciences. From 2005 until 2010, he worked on his doctoral thesis with the topic “Development of a biplanar micro multipole ion trap”. He is currently focusing on research about “Micro Energy Harvesting”.

Peter Woias has studied electrical engineering at the Technical University Munich from 1982 until 1988. He received his doctorate in ISFET-based chemical sensing from the TU Munich in 1995. From 1995 to 2000 he was a group leader on “actuators and fluidics” and later the head of the department “micromechanics, actuators and fluidics” at the Fraunhofer Institute for Microelectronic Circuits and Systems, Munich. Since July 2000 he owns a full professorship at the Laboratory for Design of Microsystems, Department of Microsystems Engineering – IMTEK, University of Freiburg, Germany. His actual fields of research include piezoelectric and thermoelectric energy harvesting, micro heat engines, microfluidic devices and systems and chemical micro process engineering.